

## Biologically Active Polymersomes from Amphiphilic Glycopeptides

Jin Huang,<sup>†,||</sup> Colin Bonduelle,<sup>§,||</sup> Julie Thévenot,<sup>§</sup> Sébastien Lecommandoux,<sup>\*,§</sup> and Andreas Heise<sup>\*,†,‡</sup>

<sup>†</sup>School of Chemical Sciences, Dublin City University, Dublin 9, Ireland

<sup>‡</sup>Technische Universiteit Eindhoven, Den Dolech 2, P.O. Box 513, 5600 MB Eindhoven, The Netherlands

<sup>§</sup>Université de Bordeaux/IPB, ENSCBP, 16 avenue Pey Berland, 33607 Pessac Cedex, France, and CNRS, Laboratoire de Chimie des Polymères Organiques (UMRS629), Pessac, France

### **S** Supporting Information

**ABSTRACT:** Polypeptide block copolymers with different block length ratios were obtained by sequential ring-opening polymerization of benzyl-L-glutamate and propargylglycine (PG) *N*-carboxyanhydrides. Glycosylation of the poly(PG) block was obtained by Huisgens cycloaddition “click” reaction using azide-functionalized galactose. All copolymers were self-assembled using the nanoprecipitation method to obtain spherical and wormlike micelles as well as polymersomes depending on the block length ratio and the nanoprecipitation conditions. These structures display bioactive galactose units in the polymersome shell, as proven by selective lectin binding experiments.

The targeted delivery of highly specific next-generation drugs such as biopharma therapeutics (peptides, proteins, and nucleic acids) requires the development of new smart drug delivery systems.<sup>1</sup> In this respect, carriers resulting from the self-assembly of amphiphilic block copolymers offer a wide scope of possibilities.<sup>2</sup> Important factors that determine the morphology obtained from these molecules are the block length ratio of the hydrophilic and hydrophobic blocks as well as the processing conditions.<sup>3</sup> Accordingly, morphologies can range from spherical to wormlike micelles and vesicles.<sup>4</sup> While micelles have been the most intensively studied and wormlike micelles have recently shown very promising long-term blood circulation, their use has mainly been limited to the loading of hydrophobic drugs.<sup>5,6</sup> Polymersomes, on the other hand, are ideally suited containers, as they can carry high payloads of both hydrophobic and hydrophilic drugs.<sup>7</sup> For targeted drug delivery, polymersomes should display biological recognition units on the surface for specific interactions with cells. For the latter, glycans (i.e., carbohydrates) are ideal candidates, as they play an important role in cell interaction and recognition.<sup>8,9</sup> Three different approaches have been explored to date for the synthesis of glycopolymeric vesicles: (1) conjugation of glycans to preformed polymersomes,<sup>10</sup> (2) formation of polymersomes from end-functionalized synthetic block copolymers,<sup>11</sup> and (3) formation of polymersomes from polymers comprising biomolecule-containing hydrophilic blocks.<sup>12</sup> The last approach favors the formation of polymersomes with highly functionalized inner and outer surfaces. This allows biomolecules to be located in deeper layers, resulting in enhanced interaction with

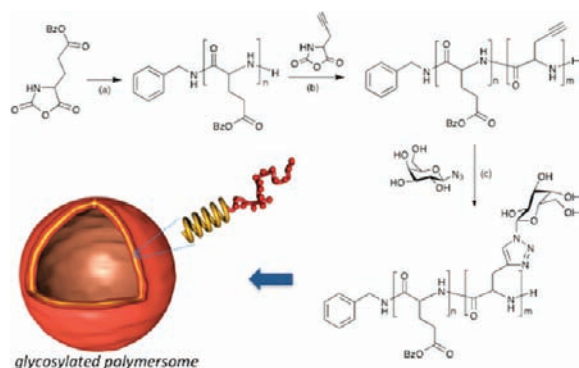
the biological target in comparison with approaches involving end-functionalized block copolymers.

As an alternative to purely synthetic polymers, polypeptide-based copolymers show considerable promise as building blocks for polymersomes.<sup>5</sup> In addition to their biodegradability, the supramolecular organization of peptides offers an opportunity to produce hierarchical structures and can also be used to promote specific “bioactivity”.<sup>13</sup> For example, it has been shown that the helical conformation of a hydrophobic peptide segment such as poly( $\gamma$ -benzyl-L-glutamate) (PBLG) is an efficient way to form and stabilize vesicles.<sup>14</sup> Block copolymers combining polypeptide and oligosaccharide blocks have previously been used to prepare glycoprotein biomimetic polymersomes.<sup>15</sup> This promising approach allowed the preparation, by chemical coupling, of dextran-*b*-PBLG and hyaluronan-*b*-PBLG. In aqueous solution, these simple glycoprotein analogues self-assemble into glycopeptidic polymersomes (glycopeptosomes) having structures and properties similar to those of viral capsids. However, this approach is not cost-effective and requires well-defined oligosaccharides. We therefore disclose the efficient synthesis of novel amphiphilic glycopeptide block copolymers and their formulation into lectin-binding polymersomes. In this design, carbohydrates that have been introduced on the side chains of the hydrophilic segment fulfill a dual function by promoting self-assembly and specific binding. The synthetic protocol, which uses controlled polypeptide synthesis and postglycosylation, and the self-assembly protocol permit extensive control over the morphology of the structures formed. Because these structures are composed entirely of amino acids and natural carbohydrates, our approach omits the use of synthetic polymers and offers a fully biocompatible system.

We propose PBLG-*b*-poly(galactosylated propargylglycine) (PBLG-*b*-PGG) copolymers as candidates for the preparation of glycopeptidic vesicles with lectin-binding galactose presented at the polymersome surface (Scheme 1). The preparation of the block copolymer was based on our previously reported synthesis of glycopeptides by Huisgens’ “click” reaction of azide-functionalized galactose to poly(propargylglycine).<sup>16</sup> The latter can easily be obtained by ring-opening polymerization of the *N*-carboxyanhydride (NCA) of propargylglycine (PG). On the basis of this synthetic strategy, amphiphilic block copolymers were obtained by sequential polymerization of

Received: October 14, 2011

Published: December 12, 2011

Scheme 1. Synthesis of PBLG-*b*-PGG Glycopeptide Block Copolymers<sup>a</sup>

<sup>a</sup>Conditions: (a) DMF, benzylamine, 0 °C; (b) DMSO, r.t.; (c) Cu(PPh<sub>3</sub>)<sub>3</sub>Br, Et<sub>3</sub>N, DMSO, 30 °C.

BLG-NCA and PG-NCA and subsequent glycosylation using the click reaction (Scheme 1). Because of the better solubility of the PBLG block, BLG-NCA polymerization was carried out first in DMF at 0 °C to prevent end-group termination.<sup>17</sup> After 4 days, BLG-NCA was completely consumed, as monitored by FTIR and NMR spectroscopy, and the PBLG macroinitiator was added to PG-NCA in DMSO at room temperature for chain extension. While the ratio of initiator to BLG-NCA was kept constant at 1:20, the ratio of PG-NCA to BLG-NCA was successively increased from 5:20 to 40:20 to obtain a library of block copolymers with increasing ratios of hydrophilic (glycosylated) to hydrophobic blocks. Analysis of the block copolymers by size-exclusion chromatography (SEC) and <sup>1</sup>H NMR spectroscopy confirmed a low polydispersity index (PDI) of ~1.1 and good agreement of the polymer composition with the monomer feed ratio [see the Supporting Information (SI)]. FTIR spectra of the block copolymers displayed amide bands typical of both  $\alpha$ -helical (1651 and 1544 cm<sup>-1</sup>) and  $\beta$ -sheet (1630 and 1513 cm<sup>-1</sup>) conformations (see the SI). As the latter band became more pronounced with increasing amount of PG, these were assigned to the  $\beta$ -sheet conformation of this block.

Glycosylation of the block copolymers was subsequently carried out with azide-functionalized galactose via Huisgens cycloaddition (Scheme 1). The success of the click reaction and the presence of galactose in the block copolymers were monitored by SEC as well as <sup>1</sup>H and <sup>13</sup>C NMR and FTIR spectroscopy (see the SI). The addition of galactose to the PG block coincided with significant increases in the molecular weights of the block copolymers (Table 1). Moreover, the complete disappearance of alkyne peaks at 73 and 80 ppm in the <sup>13</sup>C NMR spectra of the block copolymers suggests nearly quantitative glycosylation of the materials. Interestingly, the (solid-state) conformation of the block copolymers after glycosylation is different from that of the polymers before glycosylation. Amide I and II bands can be found at 1656 and 1544 cm<sup>-1</sup>, respectively, in the FTIR spectra. These positions are indicative of an  $\alpha$ -helical conformation imposed by the PBLG block. The presence of the bulky galactose moieties conjugated to the side chains in the PGG block appears to prevent the formation of  $\beta$ -sheets.

All of the block copolymers were self-assembled using the nanoprecipitation method, which consists of adding a non-solvent for the hydrophobic segment [here deionized (DI) water] to a copolymer solution (10 mg/mL) in a common

Table 1. Glycosylated Peptide Block Copolymers

block copolymer <sup>a</sup>	$M_n$ (g/mol) <sup>b</sup>		PDI <sup>b</sup>	hydrophilic weight ratio
	before glycosylation	after glycosylation		
PBLG <sub>20</sub> - <i>b</i> -PGG <sub>5</sub>	5800	9200	1.10	25%
PBLG <sub>20</sub> - <i>b</i> -PGG <sub>9</sub>	7400	9700	1.07	38%
PBLG <sub>20</sub> - <i>b</i> -PGG <sub>18</sub>	7800	11200	1.08	55%
PBLG <sub>20</sub> - <i>b</i> -PGG <sub>25</sub>	8200	11500	1.17	63%
PBLG <sub>20</sub> - <i>b</i> -PGG <sub>32</sub>	9300	16200	1.17	68%

<sup>a</sup>PBLG,  $\gamma$ -benzyl-L-glutamate; PG, propargylglycine; PGG, glycosylated poly(PG). Formulas were calculated by <sup>1</sup>H NMR analysis using the integrated peak ratios of PBLG at 5.0 ppm ( $-\text{OCH}_2\text{C}_6\text{H}_5$ ) and the combined PPG/PBLG backbone signals at 3.8–4.6 ppm ( $-\text{CHCO}-$ ), with the PBLG aromatic signal at 7.3 ppm as an internal standard.

<sup>b</sup>Determined by SEC in HFIP with PMMA standards.

solvent for both blocks (here DMSO). During this process, DMSO quickly diffused into the water phase, leading to aggregation of the hydrophobic chains and driving the self-assembly process of the amphiphilic block copolymers. The obtained morphology was generally predetermined by the molecular composition, but the system could be kinetically trapped when the kinetics of solvent diffusion was faster than the kinetics of self-assembly, leading to metastable morphologies. The material morphology could also be controlled by the order of addition (DMSO in water or water in DMSO) and the addition speed.<sup>18</sup>

Dynamic light scattering (DLS) analysis was performed after removal of DMSO by dialysis, except for samples with hydrophilic weight ratios of 25 and 38%, which underwent macroscopic aggregation. The three other samples (Table 1) appeared perfectly limpid (no macroscopic aggregation) after dialysis. Transmission electron microscopy (TEM) was used to probe the morphology directly after self-assembly. As shown in Figure 1 a–c, mixtures of spherical and wormlike structures were observed irrespective of the hydrophilic weight ratio. Changing the addition speed from a few seconds to 2 h and/or the copolymer concentration from 0.1 to 10 g/L did not significantly modify the nanoassemblies. In marked contrast, changing the order of addition (DMSO in water instead of water in DMSO) promoted the formation of spherical structures without wormlike assemblies. Small polymersomes with an average diameter of <100 nm were clearly evidenced by TEM imaging for hydrophilic weight ratios of 55 and 63% (Figure 1d,e). For PBLG<sub>20</sub>-*b*-PGG<sub>32</sub> (Figure 1f), a mixture of spherical micelles and vesicles was observed, indicating the upper hydrophilic weight ratio limit for polymersome formation with these diblock copolymers. It is worth taking into consideration that in both cases (water in DMSO or DMSO in water), the observed morphologies certainly resulted from kinetic trapping induced by the rigidity of the PBLG segment.

Vesicles made of the block copolymer PBLG<sub>20</sub>-*b*-PGG<sub>18</sub> were significantly aggregated in solution, as evidenced by TEM, atomic force microscopy (AFM), and DLS (see the SI). On the other hand, vesicles made of the copolymer PBLG<sub>20</sub>-*b*-PGG<sub>25</sub> were much more stable, allowing the determination of the radius of gyration ( $R_G$ ) and the hydrodynamic radius ( $R_H$ ) by multiangle light scattering analysis (Figure 2). As expected, the  $R_G/R_H$  ratio was found to be close to 1, attesting the formation

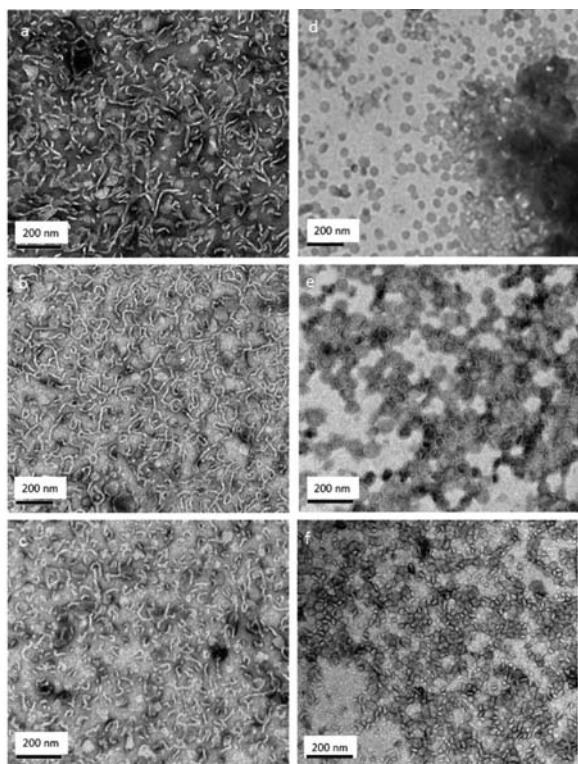


**Figure 1.** TEM images of samples obtained by instantaneously adding (a–c) water in DMSO and (d–f) DMSO in water: (a, d) PBLG<sub>20</sub>-*b*-PGG<sub>18</sub>; (b, e) PBLG<sub>20</sub>-*b*-PGG<sub>25</sub>; (c, f) PBLG<sub>20</sub>-*b*-PGG<sub>32</sub>.

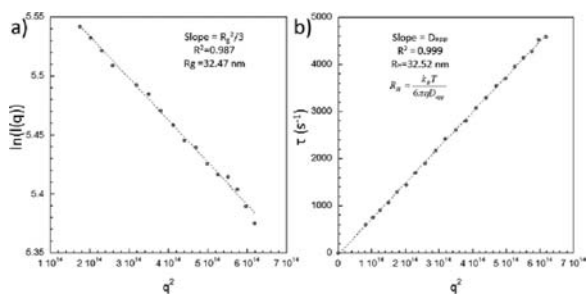


**Figure 2.** Multiangle light scattering analysis of PBLG<sub>20</sub>-*b*-PGG<sub>25</sub>. (a) Guinier plot and  $R_G$  determination. (b) Variation of decay rate vs squared scattering vector and  $R_H$  determination.

of polymersomes. High-magnification TEM imaging of the vesicles allowed good membrane visualization, the thickness being estimated as 5–10 nm. AFM analysis evidenced a diameter/height ratio in agreement with the hollow structure (Figure 3). As a result, by means of a solvent-injection method, galactosylated vesicles with small sizes and good dispersity were obtained by using (1) the appropriate block copolypeptides after galactose coupling and (2) the appropriate nanoprecipitation process and in particular the correct order of solvent addition.

The bioactivity of the glycopeptide polymersomes formed from PBLG<sub>20</sub>-*b*-PGG<sub>25</sub> copolymer was assessed by carbohydrate–lectin binding experiments. This involved mixing of the glycosylated polymersome solution with a lectin that specifically binds the sugar conjugated to the copolymer. In this case, *Ricinus communis* agglutinin (RCA<sub>120</sub>) was chosen because it is highly specific and selective for binding of galactosyl residues.<sup>19</sup> Upon the addition of different concentrations of the

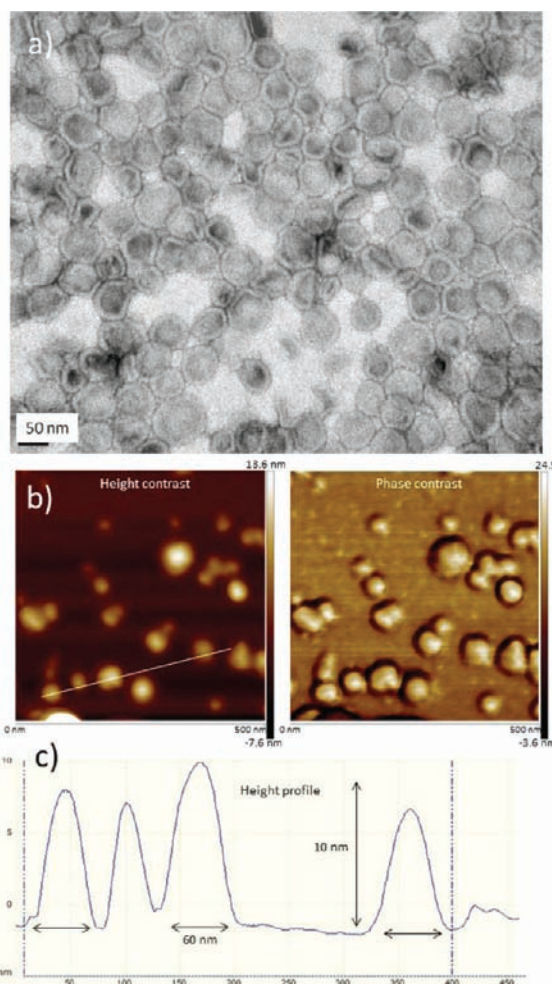


**Figure 3.** Microscopy of galactosylated polymersomes made of PBLG<sub>20</sub>-*b*-PGG<sub>25</sub>: (a) high-magnification TEM image; (b) AFM image; (c) section profile of the AFM image along the white line in (b).

glycopeptide polymersomes to the RCA<sub>120</sub> solution, instantaneous precipitation was observed. This signifies that the carbohydrate groups present at the surface of the polymersomes are available to mediate the interaction with the biological target molecules. In an attempt to quantify the interaction with the RCA<sub>120</sub>, the absorbance spectra of the polymersome/lectin solutions were recorded. As shown in Figure 4, the absorbance is highest for the greatest concentration of glycopeptide polymersomes. Furthermore, the lectin binding is so rapid that no change of absorbance was measured over time regardless of the concentration of glycosylated block copolymer. The control experiment with concanavalin A (Con A), which is selective for mannosyl and glucosyl but unable to bind galactosyl residues,<sup>19</sup> showed no significant precipitation or change in turbidity. In addition, the lectin recognition experiments were also performed using self-assembled structures obtained from the other glycopeptide block copolymers (Table 1). It was observed that all of the structures showed biological activity in these tests (see the SI). For the block copolymers with longer glycopeptide blocks, the absorbance slightly increased, although it is uncertain whether this small difference was caused by the chain length of the glycopeptide blocks or the structure of the self-assembly.

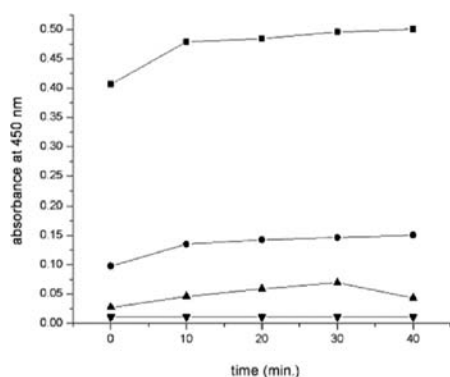


**Figure 4.** Absorbance (450 nm) of PBLG<sub>20</sub>-b-PGG<sub>25</sub> polymersomes in the presence of two different lectins in DI water: (■) lectin RCA<sub>120</sub>, glycopeptide concentration 1.0 mg/mL; (●) lectin RCA<sub>120</sub>, glycopeptide concentration 0.25 mg/mL; (▲) lectin Con A, glycopeptide concentration 1.0 mg/mL; (▼) no lectin, glycopeptide concentration 1.0 mg/mL.

In summary, we have presented a versatile and facile route to bioactive polymersomes fully based on amino acid and carbohydrate building blocks. Using controlled NCA polymerization and efficient “click” glycosylation afforded well-defined amphiphilic galactose-containing block copolymers. Depending on the block copolymer composition and the self-assembly protocol, the morphology of the structures formed could be controlled, ranging from (wormlike) micelles to polymersomes. These materials hold promise as nanosized drug carriers for targeted delivery.

## ■ ASSOCIATED CONTENT

### ● Supporting Information

Experimental procedures; NMR, FTIR, and CD spectra; lectin binding plots; additional TEM and AFM pictures; and light scattering data. This material is available free of charge via the Internet at <http://pubs.acs.org>.

## ■ AUTHOR INFORMATION

### Corresponding Author

[lecommandoux@enscbp.fr](mailto:lecommandoux@enscbp.fr); [andreas.heise@dcu.ie](mailto:andreas.heise@dcu.ie)

### Author Contributions

<sup>||</sup>These authors contributed equally.

## ■ ACKNOWLEDGMENTS

Financial support from the Science Foundation Ireland (SFI) Principal Investigator Award 07/IN1/B1792 (J.H. and A.H.) and the IUPAC Glycopeptides Project (AC-POL-09-11-25) is gratefully acknowledged. A.H. is an SFI Stokes Senior Lecturer (07/SK/B1241). The authors also thank Anne Shanahan (Dublin Institute of Technology) for help with CD measurements and Gijs J. M. Habraken (Technische Universiteit Eindhoven) for GPC measurements. The P2M program from the ESF is also gratefully acknowledged.

## ■ REFERENCES

- (1) (a) Couvreur, P.; Gref, R.; Andrieux, K.; Malvy, C. *Prog. Solid State Chem.* **2006**, *34*, 231. (b) Reischl, D.; Zimmer, A. *Nanomed. Nanotechnol.* **2009**, *5*, 8. (c) Itaka, K.; Kataoka, K. *Eur. J. Pharm. Biopharm.* **2009**, *71*, 475. (d) Du, J.; O'Reilly, R. K. *Soft Matter* **2009**, *5*, 3544.
- (2) Johnston, A. P. R.; Such, G. K.; Ng, S. L.; Caruso, F. *Curr. Opin. Colloid Interface Sci.* **2011**, *16*, 171.

- (3) Discher, D. E.; Eisenberg, A. *Science* **2002**, *297*, 967.
- (4) (a) Jain, S.; Bates, J. S. *Science* **2003**, *300*, 460. (b) Gillies, E. R.; Fréchet, J. M. J. *Chem. Commun.* **2003**, 1640.
- (5) van Dongen, S. F. M.; de Hoog, H.-P. M.; Peters, R. J. R. W.; Nallani, M.; Nolte, R. J. M.; van Hest, J. C. M. *Chem. Rev.* **2009**, *109*, 6212.
- (6) Geng, Y.; Dalhaimer, P.; Cai, S. S.; Tsai, R.; Tewari, M.; Minko, T.; Discher, D. E. *Nat. Nanotechnol.* **2007**, *2*, 249.
- (7) (a) Brinkhuis, R. P.; Rutjes, F. P. J. T.; van Hest, J. C. M. *Polym. Chem.* **2011**, *2*, 1449. (b) Massignani, M.; Lomas, H.; Battaglia, G. *Adv. Polym. Sci.* **2010**, *229*, 115. (c) Bertin, A.; Hermes, F.; Schlaad, H. *Adv. Polym. Sci.* **2010**, *224*, 167. (d) Christian, D. A.; Cai, S.; Bowen, D. M.; Kim, Y.; Pajeroski, D.; Discher, D. E. *Eur. J. Pharm. Biol.* **2009**, *71*, 463. (e) Meng, F.; Zhong, Z.; Feijen, J. *Biomacromolecules* **2009**, *10*, 197. (f) Egli, S.; Nussbaumer, M. G.; Balasubramanian, V.; Chami, M.; Bruns, N.; Palivan, C.; Meier, W. *J. Am. Chem. Soc.* **2011**, *133*, 4476.
- (8) Gamblin, D. P.; Scanlan, E. M.; Davis, B. G. *Chem. Rev.* **2009**, *109*, 131.
- (9) (a) Egli, S.; Schlaad, H.; Bruns, N.; Meier, W. *Polymers* **2011**, *3*, 252. (b) Becer, C. R.; Gibson, M. L.; Geng, J.; Ilyas, R.; Wallis, R.; Mitchell, D. A.; Haddleton, D. M. *J. Am. Chem. Soc.* **2010**, *132*, 15130. (c) Geng, J.; Mantovani, G.; Tao, L.; Nicolas, J.; Chen, G.; Wallis, R.; Mitchell, D. A.; Johnson, B. R. G.; Evans, S. D.; Haddleton, D. M. *J. Am. Chem. Soc.* **2007**, *129*, 15156.
- (10) Martin, A. L.; Li, B.; Gillies, E. R. *J. Am. Chem. Soc.* **2009**, *131*, 734.
- (11) (a) Kim, B. S.; Yang, W. Y.; Ryu, J. H.; Yoo, Y. S.; Lee, M. *Chem. Commun.* **2005**, 2035. (b) Kim, B. S.; Hong, D. J.; Bae, J.; Lee, M. *J. Am. Chem. Soc.* **2005**, *127*, 16333. (c) Toyotama, A.; Kugimiya, S. I.; Yamanaka, J.; Yonese, M. *Chem. Pharm. Bull.* **2001**, *49*, 169.
- (12) (a) Hordyjewicz-Baran, Z.; You, L.; Smarsly, B.; Sigel, R.; Schlaad, H. *Macromolecules* **2007**, *40*, 3901. (b) You, L.; Schlaad, H. *J. Am. Chem. Soc.* **2006**, *128*, 13336. (c) Schlaad, H.; You, L.; Sigel, R.; Smarsly, B.; Heydenreich, M.; Manton, A.; Mašić, A. *Chem. Commun.* **2009**, 1478. (d) Gress, A.; Smarsly, B.; Schlaad, H. *Macromol. Rapid Commun.* **2008**, *29*, 304. (e) Li, Z.-C.; Liang, Y.-Z.; Li, F.-M. *Chem. Commun.* **1999**, 1557. (f) Liang, Y.-Z.; Li, Z.-C.; Li, F.-M. *New J. Chem.* **2000**, *24*, 323. (g) Zhou, W.; Dai, X.-H.; Dong, C.-M. *Macromol. Biosci.* **2008**, *8*, 268. (h) Dai, X.-H.; Dong, C.-M. *J. Polym. Sci., Part A: Polym. Chem.* **2008**, *46*, 817. (i) Pasparakis, G.; Alexander, C. *Angew. Chem., Int. Ed.* **2008**, *47*, 4847. (j) Ercelen, S.; Zhang, X.; Duportail, G.; Grandfils, C.; Desbrières, J.; Karaeva, S.; Tikhonov, V.; Mély, Y.; Babak, V. *Colloids Surf., B* **2006**, *51*, 140. (k) Li, M.; Su, S.; Xin, M.; Liao, Y. *J. Colloid Interface Sci.* **2007**, *311*, 285.
- (13) Carlsen, A.; Lecommandoux, S. *Curr. Opin. Colloid Interface Sci.* **2009**, *14*, 329.
- (14) (a) Holowka, E. P.; Pochan, D. J.; Deming, T. J. *J. Am. Chem. Soc.* **2005**, *127*, 12423. (b) Rodriguez-Hernandez, J.; Lecommandoux, S. *J. Am. Chem. Soc.* **2005**, *127*, 2026.
- (15) (a) Schatz, C.; Louguet, S.; Le Meins, J.-F.; Lecommandoux, S. *Angew. Chem., Int. Ed.* **2009**, *48*, 2572. (b) Upadhyay, K. K.; Le Meins, J.-F.; Misra, A.; Voisin, P.; Bouchaud, V.; Ibarboure, E.; Schatz, C.; Lecommandoux, S. *Biomacromolecules* **2009**, *10*, 2802. (c) Upadhyay, K. K.; Bhatt, A. N.; Mishra, A. K.; Dwarakanath, B. S.; Jain, S.; Schatz, C.; Meins, J.-F. L.; Farooque, A.; Chandraiah, G.; Jain, A. K.; Misra, A.; Lecommandoux, S. *Biomaterials* **2010**, *31*, 2882.
- (16) Huang, J.; Habraken, G.; Audouin, F.; Heise, A. *Macromolecules* **2010**, *43*, 6050.
- (17) (a) Habraken, G. J. M.; Peeters, M.; Dietz, C. H. J. T.; Koning, C. E.; Heise, A. *Polym. Chem.* **2010**, *1*, 514. (b) Habraken, G. J. M.; Wilsens, K. H. R. M.; Koning, C. E.; Heise, A. *Polym. Chem.* **2011**, *2*, 1322.
- (18) Sanson, C.; LeMeins, J.; Schatz, C.; Brûlet, A.; Soum, A.; Lecommandoux, S. *Langmuir* **2010**, *26*, 2751.
- (19) Ambrosi, M.; Cameron, N. R.; Davis, B. G. *Org. Biomol. Chem.* **2005**, *3*, 1593.